

## Experiment Report Form

**The double page inside this form is to be filled in by all users or groups of users who have had access to beam time for measurements at the ESRF.**

Once completed, the report should be submitted electronically to the User Office via the User Portal:

<https://www.esrf.fr/misapps/SMISWebClient/protected/welcome.do>

### ***Reports supporting requests for additional beam time***

Reports can be submitted independently of new proposals – it is necessary simply to indicate the number of the report(s) supporting a new proposal on the proposal form.

The Review Committees reserve the right to reject new proposals from groups who have not reported on the use of beam time allocated previously.

### ***Reports on experiments relating to long term projects***

Proposers awarded beam time for a long term project are required to submit an interim report at the end of each year, irrespective of the number of shifts of beam time they have used.

### ***Published papers***

All users must give proper credit to ESRF staff members and proper mention to ESRF facilities which were essential for the results described in any ensuing publication. Further, they are obliged to send to the Joint ESRF/ ILL library the complete reference and the abstract of all papers appearing in print, and resulting from the use of the ESRF.

Should you wish to make more general comments on the experiment, please note them on the User Evaluation Form, and send both the Report and the Evaluation Form to the User Office.

### **Deadlines for submission of Experimental Reports**

- 1st March for experiments carried out up until June of the previous year;
- 1st September for experiments carried out up until January of the same year.

### **Instructions for preparing your Report**

- fill in a separate form for each project or series of measurements.
- type your report, in English.
- include the reference number of the proposal to which the report refers.
- make sure that the text, tables and figures fit into the space available.
- if your work is published or is in press, you may prefer to paste in the abstract, and add full reference details. If the abstract is in a language other than English, please include an English translation.



	<b>Experiment title:</b> Structural transformations affecting the size-dependent oxygen reduction reaction activity of sub-10 nm PtNi <sub>3</sub> alloy nanoparticles	<b>Experiment number:</b> CH-5004
<b>Beamline:</b> ID31	<b>Date of experiment:</b> from: 10 May 2017 to: 15 May 2017	<b>Date of report:</b> 17.10.17
<b>Shifts:</b> 15	<b>Local contact(s):</b> Jakub Drnec	<i>Received at ESRF:</i>
<b>Names and affiliations of applicants</b> (* indicates experimentalists): *Fabio Dionigi, TU Berlin *Henrike Schmies, TU Berlin *Elisabeth Hornberger, TU Berlin *Thomas Merzdorf, TU Berlin Arno Bergmann, TU berlin Peter Strasser, TU Berlin		

## Report:

In this project we have applied *in operando* wide angle X-ray scattering (WAXS) to study structural transformations which affect the stability of sub-10 nm shape selected Pt alloy nanoparticle catalysts for the oxygen reduction reaction (ORR). Among this material family, octahedral PtNi alloy nanoparticles have been reported to possess very high initial mass activity when measured by using thin film rotating disk electrode (RDE).<sup>1</sup> One of the principles used to explain their performance is based on their particular geometrical shape which exposes and maximizes the (111) surface. This surface has been observed to possess extraordinary high specific activity for single crystal with Pt<sub>3</sub>Ni composition and for this reason it is desirable to recreate at the nanometer scale.<sup>2</sup> Despite the high mass activity, morphological stability and high current density performance in membrane electrode assemblies (MEA) are still challenging.<sup>3</sup> In particular, Ni loss and other degradation processes often results in change of octahedral shape into more “rounded” or concave structures with loss of the (111) facet and lower activity.<sup>4</sup> Ni loss will also increase the Pt/Ni ratio and cause an expansion of the fcc lattice, since the lattice parameter “a” for bulk Pt is higher than the one for bulk Ni.

To study this process, we have measured *in operando* WAXS of octahedral Pt<sub>71.4</sub>Ni<sub>28.6</sub>/C and Pt<sub>66.6</sub>Ni<sub>31.9</sub>Mo<sub>1.5</sub>/C nanoparticles, in the following abbreviated as PtNi/C and PtNiMo/C. The size of the octahedral nanoparticles was ~7 nm (vertex-to-vertex) for both samples as estimated by transmission electron microscopy (TEM), which is particularly small for octahedral PtNi which often are reported having sizes of 9-12 nm. Several samples were prepared by drop casting an ink on gas diffusion layer (GDL) carbon sheets from Sigracet SGL with a platinum loading of ~50 μg<sub>Pt</sub> cm<sup>-2</sup>. WAXS was measured using our transmission cell filled with 0.1 M HClO<sub>4</sub> electrolyte. Peek foil was used as X-ray window. X-ray attenuation due to the electrolyte film was reduced significantly thanks to the high-energy X-ray radiation. First for each sample, WAXS was measured in the dry state, after inserting the electrolyte (wet state) and after activation. The activation was achieved by cycling 50 times between 0.05 V<sub>RHE</sub> and 0.925 V<sub>RHE</sub> at 100 mVs<sup>-1</sup> scan rate. Finally, a stability test was performed and WAXS measured every ~10 min. Two different protocols were used:

- Stability protocol L: 5000cycles, 100 mVs<sup>-1</sup>, 0.6-0.925 V<sub>RHE</sub>
- Stability protocol H: 2500cycles, 100 mVs<sup>-1</sup>, 0.6-1.26 V<sub>RHE</sub>

Protocol H has a potential range that extends well inside the Pt oxidation region and roughly double the one of protocol L. Accordingly, the number of cycles of H have been reduced by a factor 2 to last similarly as protocol L. “H” stands for high upper potential, 1.26 V<sub>RHE</sub>, while “L” for low, 0.925 V<sub>RHE</sub>. Preliminary results are illustrated in Figure 1, where the (220) peaks have been fitted by pseudovoigt function after background subtraction.

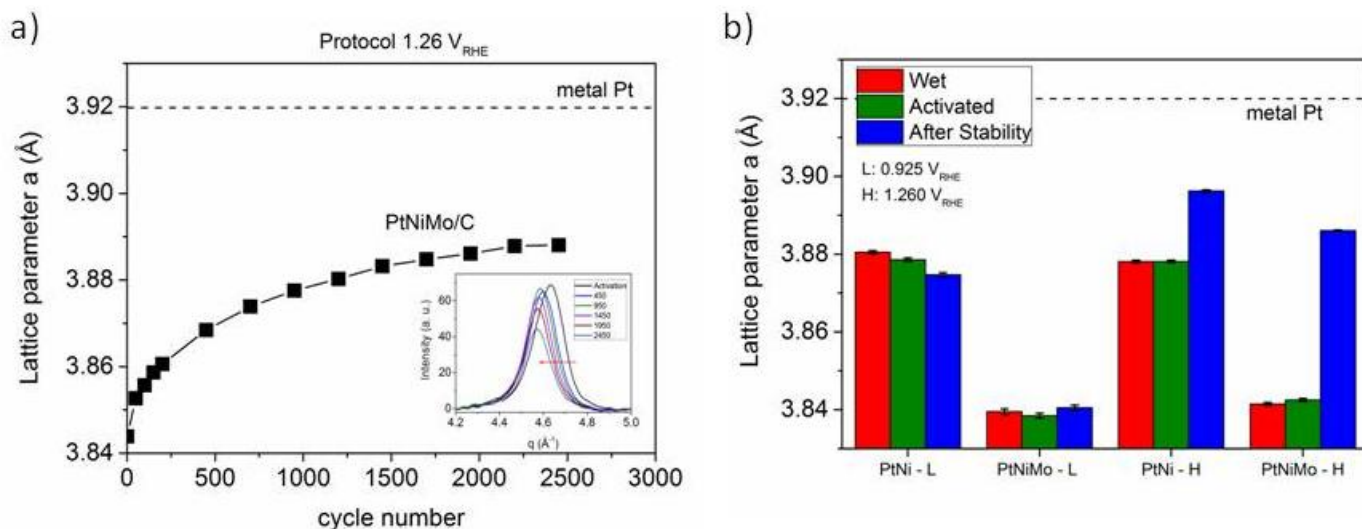


Figure 1: Lattice parameter *a* as a function of cycle number during stability protocol H for PtNiMo/C (a) and comparison of lattice parameter for wet state (red), activated (green) and after stability (blue) for PtNi and PtNiMo (b). Values for both protocol L and H are shown. In insert of (a) the (220) peak from WAXS measurements during stability is shown.

The WAXS measurements show that in protocol L where the potential is kept under control below  $\sim 1$  V<sub>RHE</sub>, (at 0.925 V<sub>RHE</sub>), both catalysts show a stable structure, with no clear change in the lattice parameter *a*. On the other end, if the upper potential is increased, for example to 1.26 V<sub>RHE</sub>, both samples show an increase in the lattice parameter, which agrees with a dominant Ni leaching. The shift is more pronounced for PtNiMo/C, which contains more Ni than PtNi/C, which might indicate that at this potential Mo is not affecting the stability behaviour, which is mainly affected by the Ni content. These measurements are in agreement with the stability loss measured by RDE by Huang et al. on similar catalysts and same upper potential limits of 1.26 V<sub>RHE</sub>.<sup>5</sup> Rietveld refinement is in progress and will further reveal differences, for example in change of crystallite sizes, occurring with different stability protocols. The analysis of the diffraction patterns measured during the stability tests will also help to understand with what rate the Ni leaching occur in the two catalysts and how quickly. In conclusion, we were able to measure in situ WAXS on highly active PtNi/C and PtNiMo/C ORR catalysts. Significant structural changes are observed when the upper potential of the stability cycles is in the platinum oxidation region, suggesting dominant Ni leaching. A deeper analysis of the data with Rietveld refinement is expected to provide additional information to clarify the mechanism and understand the causes of stability loss for sub-10 nm octahedral PtNi based alloy.

1. P. Strasser, *Science*, 2015, **349**, 379-380.
2. V. R. Stamenkovic, B. Fowler, B. S. Mun, G. F. Wang, P. N. Ross, C. A. Lucas and N. M. Markovic, *Science*, 2007, **315**, 493-497.
3. D. Banham and S. Ye, *ACS Energy Letters*, 2017, DOI: 10.1021/acseenergylett.6b00644, 629-638.
4. L. Gan, C. H. Cui, M. Heggen, F. Dionigi, S. Rudi and P. Strasser, *Science*, 2014, **346**, 1502-1506.
5. X. Q. Huang, Z. P. Zhao, L. Cao, Y. Chen, E. B. Zhu, Z. Y. Lin, M. F. Li, A. M. Yan, A. Zettl, Y. M. Wang, X. F. Duan, T. Mueller and Y. Huang, *Science*, 2015, **348**, 1230-1234.